JOURNAL OF SOLID STATE CHEMISTRY 59, 388–392 (1985)

BRIEF COMMUNICATIONS

Crystallite Size and Microstrains of Co_3O_4 Derived from CoOOH and $Co(OH)_2$

L. HERNÁN, J. MORALES, AND J. L. TIRADO

Departamento de Química Inorgánica, Facultad de Ciencias, Universidad de Córdoba, Spain

Received August 15, 1984; in revised form January 18, 1985

The variation of crystallite size and microstrains in Co_3O_4 derived from the thermal decomposition of CoOOH and $Co(OH)_2$ is studied by X-ray diffraction line broadening analysis in several crystallographic directions. The results show that the low-temperature oxide derived from CoOOH produces lower crystallite size and microstrains, due to the development of cracks in the particles instead of a porous system which is characteristic of the sample derived from $Co(OH)_2$. On the other hand, microstrains decrease and crystallite size increases with temperature for both parent compounds, but the changes are dependent on the crystallographic direction. The shape of crystallites is anisotropic at low temperature but the isotropy increases on heating, specially for the samples obtained from CoOOH. © 1985 Academic Press, Inc.

Introduction

The textural and morphological aspects of the spinel Co_3O_4 as prepared by the thermal decomposition of plate-like hydroxide and oxyhydroxide have been studied extensively by electron microscopy (*1–3*). These studies have shown that the oxide maintains the external habit of the parent material and that the axis of the plates is parallel to the [111] direction. However, little attention has been paid to structural parameters such as crystallite size and microstrains, and studies of the reactivity of this material have proved interesting.

The aim of this paper is to compare the size of crystallites of Co_3O_4 derived from the thermal decomposition of CoOOH and $Co(OH)_2$ at different temperatures. The values of crystallite size are computed for several crystallographic directions in order to obtain a qualitative evaluation of the changes in shape involving the thermal treatment of the spinel. These results are complemented by electron microscopy studies.

Experimental

The CoOOH sample was synthesized according to the method of Delaplane *et al.* (*4*). The dark brown powder suspended in water was heated at 120°C for 11 days in an autoclave Phaxe 2005 to improve the crystallinity. Cobalt(II) hydroxide was obtained by adding 0.1 *M* NaOH to a 0.1 *M* solution of $CoCl_2$ in which O_2 had been eliminated. The particles of both samples were nonporous hexagonal plates with mean diameters of 3200 and 2500 Å for $Co(OH)_2$ and

0022-4596/85 $3.00

CoOOH, respectively. The thickness of the CoOOH particles was higher, as evidenced by their pronounced opacity to electrons.

Three Co_3O_4 samples were prepared by the thermal decomposition of CoOOH under vacuum at 300, 400, and 500°C for 1 hr each. These will be henceforth referred to as A. The thermal decomposition of $Co(OH)_2$ in an oxygen atmosphere for 1 hr provided four samples at 300, 400, 500, and 600°C, referred to as B. A Co_3O_4 sample was annealed at 1000°C for 5 hr. This sample was used to obtain the instrumental X-ray profiles.

X-Ray diffraction patterns were recorded on a Philips PW 1130 diffractometer equipped with Co$K\alpha$ radiation and Fe filter. Line profiles were obtained by continuous scan at 0.125° 2θ min^{-1}. The intensities were read each 0.025° of 2θ.

The crystallite size (ε_k) and microstrains ($\langle e^2 \rangle$) were computed by the variance method (*5*). The background level was corrected by means of a computer program based in that of Edwards and Toman (*6*). Truncation and instrumental broadening were corrected according to Langford (*7*). This method was applied to the 220, 111, 400, and 511 reflections of Co_3O_4. On the other hand, crystallite size (ε_F) and microstrains ($\langle e_L^2 \rangle$) were computed by the *Warren–Averbach* method (*8*) after $K\alpha_2$ elimination by the Rachinger method and Stokes deconvolution.

The electron micrographs were alternatively obtained with a Siemens Elmiskop 102 and a Philips EM 300 instruments, working at 100 kV. Samples were dispersed in acetone by ultrasound and settled on copper grids covered with a carbon film.

Results and Discussion

The results of the X-ray diffraction line profile analysis of the Co_3O_4 samples are shown in Table I. The basis for the election of the profiles was their high peak-to-background ratio and the absence of overlapping lines. This latter requirement was not fulfilled by the maximum intensity line 311. The tails of the profiles were recorded in extension in order to obtain an adequate maximum range of scan. These values ranged between 2.6 and 4.1, expressed in FWHM units, and influenced the values of truncation error in the slope of the variance–range curves (between 2.1 and 14.0%), also the so-called "hook" effect in the cosine Fourier coefficients. However, these errors are within acceptable limits (*7*).

TABLE I

CRYSTALLITE SIZE AND MICROSTRAINS ($\times 10^3$) FOR A AND B SAMPLES

Temp (°C)	*hkl*	A samples				B samples			
		ε_k	$\sqrt{\langle e^2 \rangle}$	ε_F	$\sqrt{\langle e_L^2 \rangle}$	ε_k	$\sqrt{\langle e^2 \rangle}$	ε_F	$\sqrt{\langle e_L^2 \rangle}$
300	111	61	1.7			134	9.8		
	220	53	—	103	1.7	58	3.8	116	3.2
	400	66	2.2			64	4.4		
	511	93	5.2			108	4.1		
400	111	128	—			157	—		
	220	157	2.9	191	1.8	91	2.1	188	2.5
	400	151	3.2			97	—		
	511	106	1.1			113	—		
500	111	281	—			182	3.1		
	220	279	—	283	—	135	1.3	247	1.4
	400	287	0.9			192	2.5		
	511	293	0.1			124	1.1		
600	111					220	1.2		
	220					244	—	382	1.2
	400					284	—		
	511					177	—		

The values of apparent crystallite size (ε_k) and microstrains ($\langle e^2 \rangle$) in Table I were computed from the slope and intercept of the variance–range curves. Some of these plots are shown in Fig. 1. The values of intercept were corrected for instrumental broadening without considering the curvature error which is dependent on the unknown crystallite shape. However, this error may be ignored (*7*). On the other hand, the values of size coefficients (A_L^S) and microstrains ($\langle e_L^S \rangle$) were obtained from the intercept and slope of the Warren–Aver-

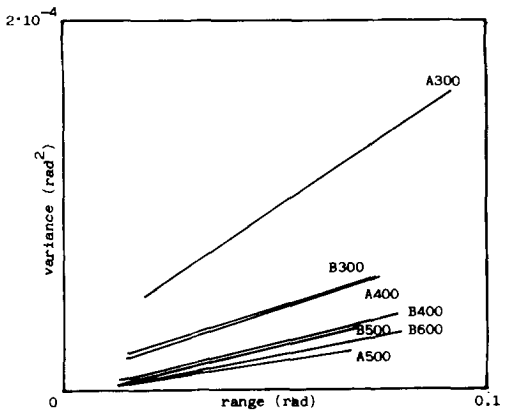

FIG. 1. Variance-range plots for the 111 reflection of Co_3O_4 (f profiles).

bach plots, as shown in Fig. 2. ε_F was computed from the derivative $dA_L^S/dL|_{L\to 0}$.

The results in Table I show that the low-temperature products A300 and B300 are of small low crystallite size and have a high microstrain content, independent of the method used in the analysis. In addition, the values of ε_k and ($\langle e^2 \rangle$) depend on the crystallographic direction, thus indicating an important anisotropy of the products. If these two samples are compared, there are noticeable differences. Thus, crystallite size and microstrains are higher for B300 and the anistropy is not equivalent. In this way, the highest value of ε_k for B300 is that computed from the 111 line, in contrast to the A300 sample.

These differences may be examined in light of the electron micrographs in Fig. 3. Both samples maintain the external plate-like morphology of the parent hydroxide but the A samples show cracks in the particle surface, while a different porous system is observed for B300. The presence of cracks may be responsible for the low values of crystallite size and for the strain relief process for A300 as pointed out in (*3*).

It should be noted that these results differ from those reported by Figlarz *et al.* (*3, 9*). These authors indicate that the transformation of a CoOOH sample with irregular porosity to Co_3O_4 causes the development of a regular porous system which is similar to that observed after the reaction $Co(OH)_2 \rightarrow CoO$, that remains after the conversion $CoO \rightarrow Co_3O_4$. The presence of cracks and the above-mentioned differences may show that the classification of both processes in the same group is valid only for samples with the textural characteristics and origin reported in (*9*).

As the temperature of preparation increases, the size of the crystallites of Co_3O_4 derived from CoOOH increase progressively and the differences between the broadening of the lines decrease. These observations are consistent with an intragranular sintering process which is accompanied by a change in crystallite shape or in the parameters that define a certain irregular shape.

An analysis of crystallite shape may be performed by the use of the Scherrer constants K_k (*10, 11*). As the shape of crystallites is unknown, the direct comparison of

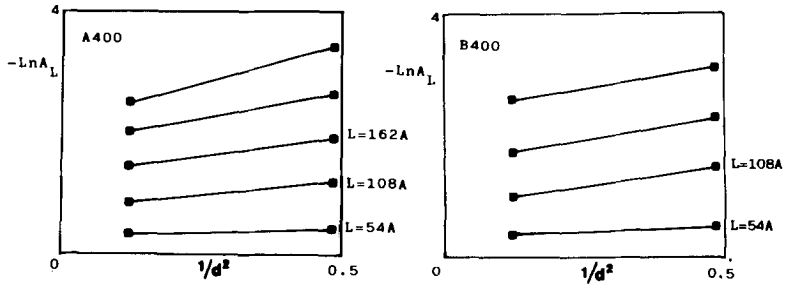

FIG. 2. Warren–Averbach plots for the 220 and 440 lines of Co_3O_4 obtained at 400°C.

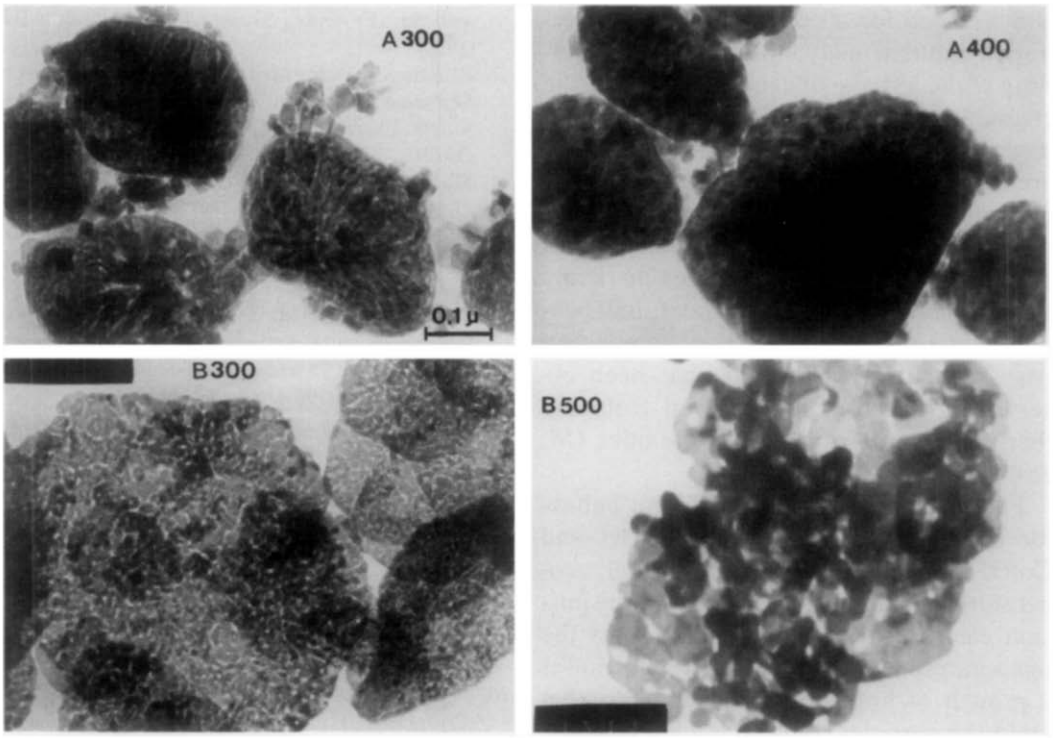

FIG. 3. Electron micrographs of Co_3O_4 obtained at different temperatures.

K_k cannot be used, but the ratios of the Scherrer constants may be computed by

$$\varepsilon_k(h_1k_1l_1)/\varepsilon_k(h_2k_2l_2) = K_k(h_2k_2l_2)/K_k(h_1k_1l_1). \quad (1)$$

If the experimental ratios are compared with the theoretical quotients corresponding to regular shapes of crystallites (*10*), it is not possible to ascribe a cube, tetrahedron, or octahedron to the crystallite shape of A300, A400, or A500. An irregular shape of crystallites has also been reported for other materials with cubic structure (*12–14*).

On the other hand (*12, 13*), it has been pointed out that a cylindric or prismatic shape can be found in cubic crystallites. However, the analysis of this possibility is restricted by the lower symmetry of these shapes which causes a superposition of several profiles at the same Bragg angle that may not be broadened equally, for example, the $\bar{1}11$, $1\bar{1}1$, and $11\bar{1}$ profiles (*12*).

Similarly, the ratios of K_k are not consistent with a regular crystallite shape for the B samples. Moreover, the electron micrographs in Fig. 3 provide no additional information on the shape of crystallites of the A or B samples, but the values of crystallite size in Table I are in accordance with the size of the grains that construct the network connecting the pores or cracks.

The most relevant aspect of the results in Table I is the different behavior with temperature of the crystallites of A and B samples. In this respect, the differences between the crystallographic directions for each temperature are higher for the B samples and B600 shows higher anisotropy than A500, probably due to the different thickness of the particles of both parent compounds. Although the growth of crystallites

is developed for all crystallographic directions simultaneously, the different anisotropy of the initial oxide may account for the characteristic behavior of each set of samples, probably due to the different surface areas exposed to the contact with other crystallites.

On the other hand, the strain content of both types of samples decreases markedly throughout the thermal treatment, independent of the method used in the computation (see Table I). This behavior has been observed in other oxides derived from the thermal decomposition of hydroxides (*15, 16*).

Further evidence of the different behavior of Co_3O_4 derived from CoOOH and $Co(OH)_2$ is obtained when the higher temperature samples are observed by transmission electron microscopy (Fig. 3). As the temperature increases, the B samples suffer a growth of both pores and domains that build the particles, but the thickness of the particles remains almost unaltered below 600°C. From 500 to 600°C, the change is more noticeable. On the other hand, the A samples increase their thickness progressively as it is evidenced by the continuous loss of transparency to electrons.

References

1. D. COLAITIS, F. FIEVET-VINCENT, J. GUENOT, AND M. FIGLARZ, *Mater. Res. Bull.* **6,** 1211 (1971).
2. R. AMMAN, V. FEITKNECHT, AND R. GIOVANOLI, Septieme Congres International de Microscopie Electronique, p. 467, Grenoble, France (1970).
3. M. FIGLARZ, J. GUENOT, AND F. FIEVET-VINCENT, *J. Mater. Sci.* **11,** 2267 (1976).
4. R. G. DELAPLANE, J. A. IBERS, J. R. FERRARO, AND J. J. RUSH, *J. Chem. Phys.* **50,** 1920 (1964).
5. J. I. LANGFORD AND A. J. C. WILSON, *in* "Crystallography and Crystal Perfection" (G. N. Ramachandran, Ed.), p. 207, Academic Press, New York/London (1963).
6. H. J. EDWARDS AND K. TOMAN, *J. Appl. Crystallogr.* **4,** 332 (1971).
7. J. I. LANGFORD, *J. Appl. Crystallogr.* **15,** 315 (1982).
8. B. E. WARREN AND B. L. AVERBACH, *J. Appl. Phys.* **23,** 497 (1952).
9. J. GUENOT, F. FIEVET-VINCENT, AND M. FIGLARZ, *in* "Reactivity of Solids" (J. Wood, O. Linqvist, C. Hegelsson, and N. G. Vannerberg, Eds.), p. 415, Plenum, New York (1977).
10. J. I. LANGFORD AND A. J. C. WILSON, *J. Appl. Crystallogr.* **11,** 102 (1978).
11. J. I. LANGFORD AND D. LOUER, *J. Appl. Crystallogr.* **15,** 20 (1982).
12. J. C. NIEPCE AND G. WATELLE, *J. Mater. Sci.* **13,** 149 (1978).
13. P. DUMAS, N. EA, J. C. NIEPCE, AND G. WATELLE, *J. Solid State Chem.* **27,** 317 (1979).
14. F. FIEVET AND M. FIGLARZ, *J. Catal.* **39,** 350 (1975).
15. F. FIEVET P. GERMI, F. DE BERGEVIN, AND M. FIGLARZ, *J. Appl. Crystallogr.* **12,** 387 (1979).
16. J. MORALES, J. L. TIRADO, AND M. MACIAS, *J. Solid State Chem.* **53,** 303 (1984).